# Superconducting and normal-state interlayer exchange coupling in $La_{0.67}Sr_{0.33}MnO_3$-$YBa_2Cu_3O_7$-$La_{0.67}Sr_{0.33}MnO_3$ epitaxial trilayers

K. Senapati and R. C. Budhani*

*Department of Physics, Indian Institute of Technology Kanpur, Kanpur-208016, India*

The issue of interlayer exchange coupling in magnetic multilayers with a superconducting spacer is addressed in $La_{0.67}Sr_{0.33}MnO_3$ (LSMO)-$YBa_2Cu_3O_7$ (YBCO)-$La_{0.67}Sr_{0.33}MnO_3$ (LSMO) epitaxial trilayers through resistivity, ac susceptibility, and magnetization measurements. The ferromagnetic LSMO layers possessing in-plane magnetization suppress the critical temperature ($T_c$) of the $c$-axis oriented YBCO thin film spacer. The superconducting order, however, survives even in very thin layers (thickness $d_Y \sim 50$ Å, $\sim$ four unit cells) at $T < 25$ K. A predominantly antiferromagnetic exchange coupling between the moments of the LSMO layers at fields <200 Oe is seen in the normal as well as the superconducting states of the YBCO spacer. The exchange energy $J_1$ ($\sim 0.08$ erg/cm$^2$ at 150 K for $d_Y = 75$ Å) grows on cooling down to $T_c$, followed by truncation of this growth on entering the superconducting state. The coupling energy $J_1$ at a fixed temperature drops exponentially with the thickness of the YBCO layer. The temperature and $d_Y$ dependencies of this primarily nonoscillatory $J_1$ are consistent with the coupling theories for systems in which transport is controlled by tunneling. The truncation of the monotonic $T$ dependence of $J_1$ below $T_c$ suggests inhibition of single-electron tunneling across the $CuO_2$ planes as the in-plane gap parameter acquires a nonzero value.

## I. INTRODUCTION

The oscillatory nature of exchange coupling between two ferromagnetic (FM) layers separated by a metallic but non-magnetic (NM) spacer as a function of the spacer thickness $d_n$ is now well established in a variety of systems.[1–7] It is generally agreed that the coupling is driven by the Rudderman-Kittel-Kasuya-Yoshida (RKKY) type exchange through the conduction electrons of the spacer.[1] The period of oscillations predicted by the theories of exchange coupling is directly related to the extremal wave vectors connecting opposite sides of the Fermi surface (FS) of the spacer material in the direction of the layer growth. Clearly, the nature of the Fermi surface of the spacer plays a key role in interlayer exchange. Šipr and Györffy[8] first suggested that an experiment in which the Fermi surface could be changed while keeping all other material parameters the same would allow a direct test of the exchange coupling theories based on extremal wave vectors of the FS. They proposed the use of a superconducting (SC) spacer in which an isotropic gap opens up at the FS on cooling below the critical temperature $T_c$. The zero-temperature numerical calculations of Šipr and Györffy[8] show that the oscillatory coupling is strongly damped in the presence of a superconducting gap. Similarly, the analytical results of de Melo[9,10] show that at $\Delta/T \gg 1$, the coupling decays exponentially as $\exp(-k_{F_s} d_s \Delta E_F)$, where $k_{F_s}$, $d_s$, $\Delta$, and $E_F$ are the Fermi wave vector, spacer thickness, gap parameter, and Fermi energy, respectively. Near $T_c$, the large thermally excited quasiparticle density compensates for the loss of coupling seen at low temperatures.

Experimental verification of these predictions is, however, constrained by several material related factors. First of all, since the oscillatory coupling is seen only when the spacer thickness is small ($\leqslant 130$ Å), one must ensure that superconductivity survives in such thin spacers in the presence of the strong pair-breaking effects of the ferromagnetic boundaries. Naturally, short coherence length $\xi_0$ and high critical temperature $T_c$ of the superconductor and small exchange energy of the ferromagnet are the desirable features to see the effect. In addition, one must also ensure that the interfaces between the ferromagnetic and superconducting layers are atomically smooth.

The doped Mott insulators of the perovskite oxide family meet some of these material specifications. For example, $YBa_2Cu_3O_7$ (YBCO) superconductor and $La_{0.67}Sr_{0.33}MnO_3$ (LSMO) ferromagnets can be grown epitaxially on top of each other. The cuprate has anisotropic but short coherence length and a high $T_c$, whereas the manganite with a Curie temperature of $\approx 360$ K has relatively small exchange energy J ($\sim 1$ meV) as compared to the J of 3d transition-metal ferromagnets such as Fe and Co which are strong pair breakers.[11] However, the cuprates also pose interesting challenges, such as the nodal gap parameters $\Delta$ and anomalous $c$-axis transport, not present in elemental superconductors. Reported measurements on high-$T_c$ superconductor (HTSC) manganite heterostructures have primarily focused on the suppression of $T_c$,[12–14] spin injection,[15–17] and the effects of magnetoresistance.[18,19] Recently, the aspect of exchange coupling across HTSC layers has been addressed by Przyslupski *et al.*[20] using $(La_{0.67}Sr_{0.33}MnO_3)_n/(YBa_2Cu_3O_7)_m$ multilayers where $n=16$ unit cells, and $m$ varies from 1 to 8 unit cells. Measurements of field-cooled (FC) and zero-field-cooled (ZFC) magnetization loops in these samples reveal exchange biasing effects, which have been argued to be an indicator of interlayer exchange coupling. However, this work also attributes the shift of the FC and ZFC loops to antiferromagnetism in LSMO. Here it needs to be pointed out that these multilayers have been deposited on $LaAlO_3$ substrates, which introduce large compressive stress in LSMO and YBCO epitaxial films due to its smaller lattice

parameter ($\sim 3.79$ Å). In addition, $LaAlO_3$ is a heavily twinned material. Since both these factors are known to affect magnetic anisotropy of LSMO (Ref. 21) and superconducting properties of YBCO,[22] intrinsic behavior of FM-SC-FM structure is likely to get masked by such stress- and interface-related effects. Further, the interface-related nonintrinsic behavior is likely to get accentuated in superlattices due to the presence of a large number of interfaces in such structures.

Here we report the magnetic behavior of LSMO-YBCO-LSMO trilayers, synthesized on [001] $SrTiO_3$ substrates. The lattice parameter of $SrTiO_3$ ($\sim 3.91$ Å) compares well with the lattice parameter of $L_{0.67}Sr_{0.33}MnO_3$ ($\sim 3.89$ Å) and the average ab-plane lattice spacing of $YBa_2Cu_3O_7$ ($\sim 3.85$ Å). The scope for a stress-free layer-by-layer growth has been improved further through special chemical treatment of the substrate.[23] We first describe the magnetic behavior of plane LSMO films of various thickness. High-quality epitaxial layers of LSMO showing a soft magnetic character and in-plane anisotropy were integrated with YBCO in a trilayer form and the superconducting critical temperature of such structures was measured. The suppression in $T_c$ has been attributed to the pair-breaking effects at the FM-SC interface. Finally, the issue of interlayer exchange coupling has been addressed through measurements of ZFC in-plane magnetization loops over a broad range of temperatures. These measurements reveal a long-range antiferromagnetic coupling between LSMO layers decaying exponentially with the thickness of the YBCO spacer.

## II. EXPERIMENT

Thin films of LSMO, and trilayers of LSMO-YBCO-LSMO and $PrBa_2Cu_3O_7$-$YBa_2Cu_3O_7$-$PrBa_2Cu_3O_7$ (PBCO-YBCO-PBCO) were deposited on chemically polished [001] oriented $SrTiO_3$ substrates. A multitarget pulsed laser deposition technique based on KrF excimer laser ($\lambda = 248$ nm) was used to deposit the films and trilayers at 800 °C and 200 mTorr $O_2$ partial pressure.[24] Since the growth conditions for all three oxides were identical, the trilayers were deposited sequentially without changing the process parameters. A slow deposition rate ($\sim 1$ Å/s) established through several calibration runs was used to realize a layer-by-layer growth of LSMO, PBCO, and YBCO. While for the plane LSMO films we have studied the changes in transport and magnetic properties as a function of thickness from 50 Å to 1100 Å, the thickness of each LSMO layer in LSMO-YBCO-LSMO trilayers was fixed at 300 Å, and the thickness of the cuprate was varied from 50 Å to 300 Å. For the PBCO-YBCO-PBCO trilayers, a constant PBCO layer thickness of 100 Å was used. The crystallographic structure of the films was characterized with $\theta-2\theta$ x-ray diffraction. The SC and FM critical temperatures of the films were established through resistivity $\rho(T)$, ac susceptibility $\chi(T)$, and magnetization M(T) measurements. We have used a home-built micro-Hall-probe based ac susceptometer[25] for detailed measurements of vortex dynamics in these films.[24] The measurements of resistivity in the temperature range of 2 K–370 K were carried out in the standard four-probe geometry. A superconducting
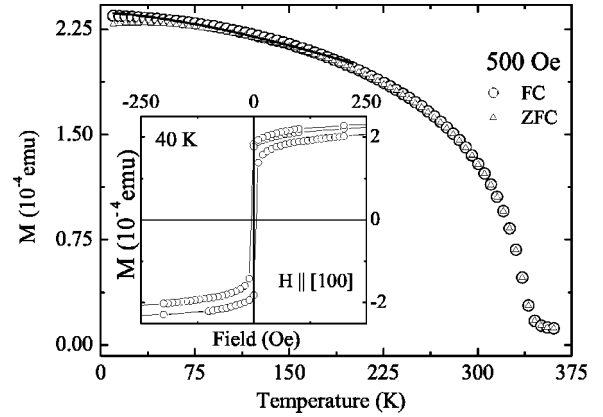


FIG. 1. Zero-field-cooled ($\triangle$) and field-cooled ($\bigcirc$) magnetization of a 600-Å-thick film of $La_{0.67}Sr_{0.33}MnO_3$ measured with a 500 Oe in-plane field directed along the [100] axis. The solid line is a fit to the field-cooled curve using the Bloch law [Eq. (1)] for the decay of magnetization at $T \ll T_c$. Inset: Zero-field-cooled hysteresis loop of the same film measured at 40 K in the same configuration as the measurement of $M(T)$.

quantum interference device (SQUID) based magnetometer (MPMS-XL5) operated in the RSO mode for higher sensitivity was used for detailed measurements of zero-field-cooled and field-cooled magnetization and M-H loops. The magnetic field in these measurements was in the plane of the film, aligned along one of the principal axes ([100] or [010]). Measurements were also performed with the field in the [110] direction to check for the in-plane anisotropy of magnetization.

## III. RESULTS

### A. Magnetic ordering in thin $La_{0.67}Sr_{0.33}MnO_3$ films

Figure 1 shows the ZFC and FC magnetization of a 600-Å-thick LSMO film measured at 500 Oe. The onset of spontaneous magnetization at $\sim 350$ K on cooling marks the Curie temperature of the sample. The ZFC and FC branches of magnetization in granular and multidomain magnetic films of large coercivity show a pronounced bifurcation at lower temperatures. In the present case, however, the two branches nearly superimpose down to the lowest temperature. This feature indicates the growth of a defect-free magnetic film of low coercivity. We analyze the temperature dependence of the FC magnetization in the framework of the Bloch theory for decay of magnetization due to excitation of spin waves.[26] The drop in saturation magnetization is predicted to be of the form

$$M_s(T)/M_s(0) = 1 - AT^{3/2}. \qquad (1)$$

Here $M_s(0)$ is the saturation magnetization at $T=0$, and the coefficient $A$ is expressed as $(C/S)(k_B 2JS)^{3/2}$, where $C = 0.059$ for a simple cubic magnetic lattice, S the total spin, and J the exchange integral which is given by the formula $k_B T_c / J = (5/96)(Z-1)[11S(S+1)-1]$ of Rushbrooke and Wood.[27] An excellent fit to the magnetization at $T \ll T_{Curie}$ is seen with a dependence of the type $1 - AT^{3/2}$, when the aver-
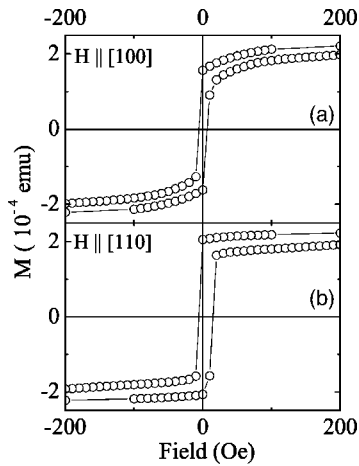
FIG. 2. Zero-field-cooled magnetization loops at 100 K measured with in-plane applied field along the [100] [panel (a)] and [110] [panel (b)] directions. In both cases, the data are corrected for a small diamagnetic contribution from the STO substrate.



FIG. 3. Resistivity $[\rho(T)]$ of LSMO films deposited on STO in the temperature range of 2 K–370 K. Thickness of the films varies from 100 Å to 350 Å. Inset shows a magnified view of the low-temperature section of the $\rho(T)$ curves. These data have been normalized with respect to the resistivity at 10 K in order to emphasize the upturn in the resistivity of the thinnest films.

age spin S (=1.835) per Mn site is used. The exchange energy deduced from the fits is ~2 meV, while the exchange energy of the strong ferromagnets like Fe is ~5.5 meV deduced from a Bloch constant of ~$3.6 \times 10^{-6}$ deg$^{-3/2}$.[26]

In order to check for a preferred in-plane axis of magnetization, we have measured the hysteresis loops with the external field aligned along the [100] and [110] directions of the [001] oriented films. Results of this measurement are shown in Figs. 2(a) and 2(b). A perfect hysteresis loop with the remanant magnetization ($M_r$) equal to $M_s$ is seen when the field is along [110], whereas in the case of H‖[100] [Fig. 2(a)], $M_r = M_s/\sqrt{2}$. This observation clearly indicates that [110] is the easy axis of magnetization and [100] is the hard axis. However, the small value of the switching field suggests that the energy barrier for rotation of magnetization is not large. This result is consistent with the earlier measurements of magnetization loops in films of LSMO deposited on STO substrates.[28,29] The square hysteresis loops seen in the figure further suggest that these films are magnetically quite soft. The behavior of magnetization in LSMO films deposited on LAO is quite different. The preferred direction of magnetization is perpendicular to the film plane in this case.[21,30,31]

Unlike the other double exchange manganites such as La$_{0.67}$Ca$_{0.33}$MnO$_3$, the resistivity of LSMO with 30–40% Sr is metallic in the paramagnetic state.[32] This metallic conduction is seen in our films as well. The resistivity of these films at room temperature is low (~2 mΩ cm), and remains metallic down to 2 K. Figure 3 displays the zero-field resistivity of LSMO films spanning over a thickness range of 100 Å–350 Å in the temperature window of 2 K–370 K. The paramagnetic metallic phase above $T_{Curie}$, which transits to a ferromagnetic metallic phase at $T < T_{Curie}$, is clearly identifiable for all films. $T_{Curie}$ acquires the near bulk value (~350 K) for films thicker than 200 Å, while thinner films show a slight drop in the Curie temperature. The resistivity at the lowest temperature normalized with respect to its value at 10 K is shown in the inset of Fig. 3. A small upturn in resistivity, which can be attributed to weak localization and
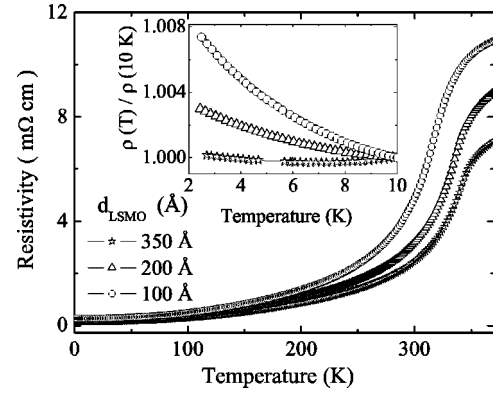
electron-electron interaction effects in 2D, is observed only for the thinnest films (≤200 Å). These features indicate the growth of a high-quality thin film of LSMO. The magnetic and electrical characteristics of LSMO dominate the behavior of $\rho(T)$ and $M(T)$ in LSMO-YBCO-LSMO trilayers at $T > 100$ K as described in the following section.

### B. Superconductivity in LSMO-YBCO-LSMO trilayers

In the inset of Fig. 4(a), we plot the magnetization and resistivity of an LSMO-YBCO-LSMO trilayer with YBCO layer thickness ($d_Y$) of 100 Å. At $T \leq 360$ K, a metallic behavior is evident in the resistivity plot. This becomes pronounced at $T < T_{Curie}$. At lower temperatures, however, the resistance of the sample drops to zero as the current path is shorted by the superconducting YBCO layer. Correspondingly, there is a nonzero diamagnetic contribution to magnetization due to the Meissner effect. In trilayers with thicker YBCO film, the magnetization actually crosses the zero line and becomes negative. This is seen in Fig. 4(b), where we have plotted the ZFC magnetization of some trilayers with different YBCO thickness. The superconducting transition temperature ($T_c$) in these heterostructures is a strong function of YBCO layer thickness. In Fig. 4(a), we show the variation of $T_c$ as a function of $d_Y$ in LSMO-YBCO-LSMO trilayers. In order to estimate the effects of magnetic boundaries on $T_c$, we have also measured the superconducting transition temperature of PBCO-YBCO-PBCO trilayers. Results of these measurements are also shown in Fig. 4(a). For this nonmagnetic system, the $T_c$ drops as the thickness of the YBCO layer ($d_Y$) is reduced. The variation of $T_c$ with $d_Y$ in PBCO-YBCO-PBCO multilayers has been studied extensively by several groups, and various reasons have been given for the drop.[33–35] These include interfacial stress, a drop in $c$-axis coupling of the condensate as the number of CuO$_2$ planes is reduced, etc. However, the effect of uniaxial stress applied along the $a$ axis and $b$ axis of the YBCO crystal on its $T_c$ is nearly equal and opposite.[36] This result rules out any direct effect of the lattice mismatch induced stress on $T_c$. However,
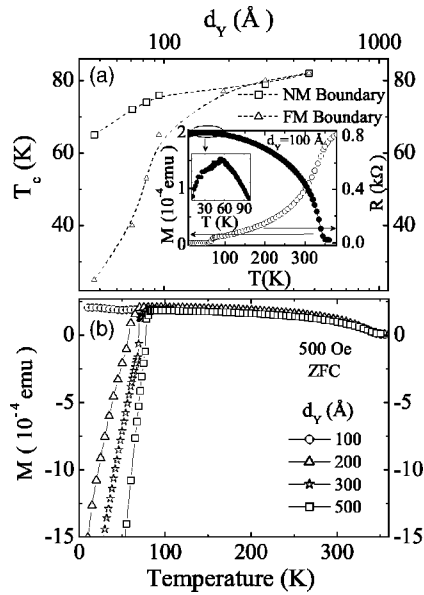
FIG. 4. Panel (a): $T_c$ (open symbols) plotted as a function of $d_Y$ in LSMO-YBCO-LSMO and PBCO-YBCO-PBCO trilayers. Inset shows $R(T)$ and zero-field-cooled $M(T)$ of an LSMO-YBCO-LSMO sample with $d_Y=100$ Å. An enlarged view of $M(T)$ near $T_c$ is also shown. Panel (b) Temperature dependence of the zero-field-cooled magnetization of LSMO-YBCO-LSMO trilayers with 100-, 200-, 300-, and 500-Å-thick SC layers. The measurement field of 500 Oe was applied along the [100] direction in the plane of the films.

Varela *et al.*[34] have shown that the overall stress pattern also gives rise to very significant and nonuniform changes within a YBCO unit cell, which may reduce the hole concentration in the $CuO_2$ planes located close to the interfaces. We may write this interface-driven reduction in $T_c$ as $\Delta T_c(d_Y)_{interface}$. Since the lattice parameters of $La_{0.67}Sr_{0.33}MnO_3$ and $PrBa_2Cu_3O_7$ are identical within 0.5%, we assume the effect of the interface on $T_c$ to be similar for YBCO films sandwiched between the LSMO layers. The LSMO layers, however, also affect the $T_c$ through pair breaking. We can therefore argue that the larger drop in $T_c$ of LSMO-YBCO-LSMO trilayers of a given $d_Y$ as compared to the $T_c$ of PBCO-YBCO-PBCO of the same $d_Y$ is due to the magnetic pair-breaking effects. A rigorous treatment of pair-breaking effects of a ferromagnetic film deposited on top of a superconductor requires solution of the Usadel equation for a different degree of interface transparency for Cooper pair tunneling.[37,38]

### C. Magnetic coupling in LSMO-YBCO-LSMO trilayers

Having established the existence of ferromagnetic and superconducting orders in these trilayers, we now discuss the behavior of interlayer magnetic coupling between the LSMO layers separated by YBCO below and above the $T_c$. Figure 5 shows a series of M-H loops of an LSMO-YBCO-LSMO trilayer with $d_Y=100$ Å taken at various temperatures with the external magnetic field aligned along the [100] direction. In the loops measured at $T>100$ K, one can easily identify a
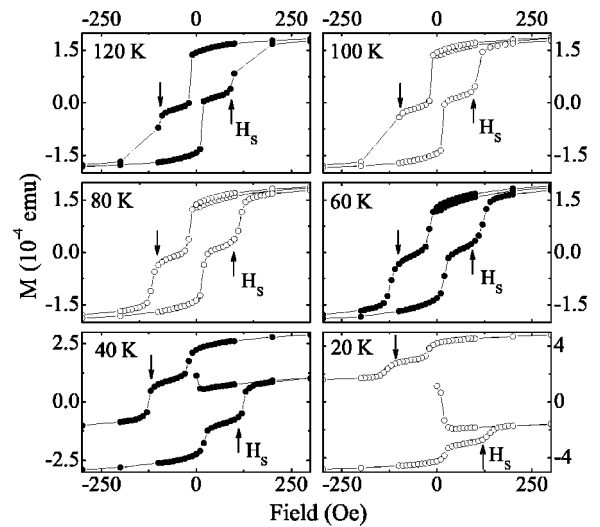


FIG. 5. Low-field section of isothermal hysteresis loops of an LSMO-YBCO-LSMO trilayer with a 100 Å YBCO interlayer, measured at 20, 40, 60, 80, 100, and 120 K. All measurements were performed on zero-field-cooled samples and with in-plane applied field along the [100] direction. The switching field has been marked as $H_s$ (see text for details).

critical field $|H_s|$ up to which the magnetic moment of the trilayer remains close to zero, and then quickly achieves the saturation value once the field [H] exceeds. $|H_s|$. The magnetization of the sample below the superconducting transition drops rapidly at low fields because of the diamagnetic signal from the YBCO layer. The reverse branch of the hysteresis loops shows a large irreversibility due to pinning of the magnetic flux. However, the ferromagnetic component of the magnetization is also found to persist in the superconducting state. A careful look at the magnetizing branches of panels (c), (d), and (e) clearly reveals the characteristic field $H_s$ below which the magnetization remains nearly constant. A similar behavior of the hysteresis, both above and below $T_c$, is seen in trilayers with a different YBCO layer thickness. The M-H loops of some samples at 100 K are shown in Fig. 6.

A straightforward explanation for the existence of $H_s$ can be given by invoking antiferromagnetic exchange coupling between the LSMO layers separated by normal and superconducting YBCO. Earlier measurements of magnetization in superlattices of ferromagnetic manganites and nonmagnetic but metallic $LaNiO_3$ have revealed indirect coupling mediated by the conduction electrons of the spacer.[6,7] This coupling is oscillatory with the thickness of the spacer. However, before proposing such a fundamental mechanism, we must rule out some rather mundane processes, which could lead to a similar effect. First of all, the interfaces of perovskite oxides based multilayers have an inherent stereochemical disorder even when they are atomically sharp.[39] This disorder is caused by a change in the nearest-neighbor environment of the magnetically active ions, and can lead to random pinning of their moment. While a gradual depinning of these moments with the increasing field would lead to deviations from a square hysteresis loop typical of a soft magnet such as LSMO, it is not likely to result in the M-H
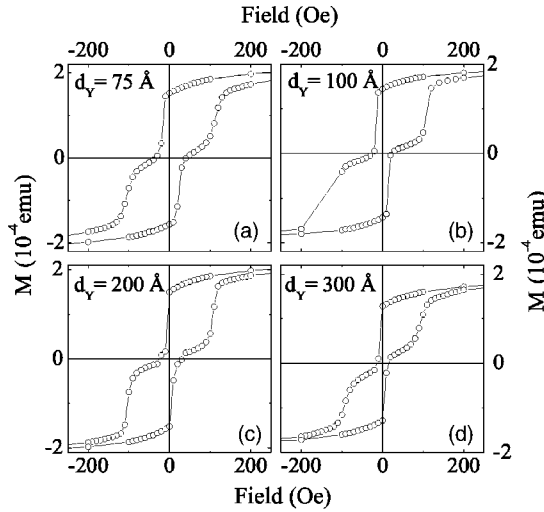
FIG. 6. Panels (a), (b), (c), and (d) display the results of isothermal magnetization measurements at 100 K for trilayers with 75-, 100-, 200-, and 300-Å-thick YBCO interlayers, respectively. The measurement field was directed along the [100] direction in the plane of the trilayers. The low-field region is magnified in order to emphasize the antiferromagnetic coupling between the LSMO layers below 200 Oe.

loops seen in Figs. 5 and 6. One may also argue that the uncompensated copper spins at the interface help stabilize this random state. In order to rule out these possibilities, we have measured the M-H loops of LSMO-PBCO-LSMO trilayers. In Figs. 7(a)–7(c), we compare the magnetization curves of a 600-Å-thick single-layer LSMO film, a LSMO-PBCO-LSMO trilayer, and a LSMO-YBCO-LSMO trilayer. In all three cases, the measuring field was along the [100] direction. Figure 7(d) shows the M-H loop of the LSMO-
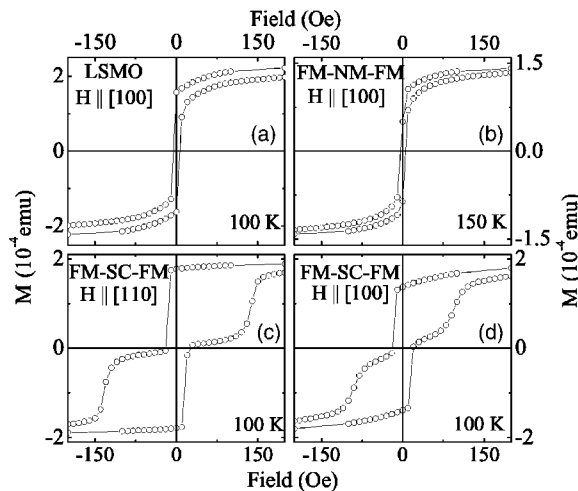


FIG. 7. A comparative view of the magnetization behavior of a 600 Å LSMO film [panel (a)], LSMO-PBCO-LSMO trilayer with 300 Å PBCO [panel (b)], and LSMO-YBCO-LSMO trilayer with 300 Å YBCO [panel (c)]. The external magnetic field was in the plane of the film and directed along the [100] axis. Panel (d) shows the magnetization while the field was applied along the [110] direction for the LSMO-YBCO-LSMO trilayer. All the curves were corrected for a small diamagnetic response of the substrate.

YBCO-LSMO trilayer measured with H∥[110] for comparison. It is evident from these data that the hysteresis with the characteristic magnetizing field $H_s$ is seen only in the case of LSMO-YBCO-LSMO trilayers. This observation rules out the role of uncompensated copper spins, as these factors are present in LSMO-PBCO-LSMO as well. Some signatures of the type of M-H curve seen in Figs. 5 and 6 have also been observed by Przyslupski *et al.*[20] in $La_{0.67}Sr_{0.33}MnO_3$-$YBa_2Cu_3O_7$ superlattices with thin ($\sim$60 Å) LSMO layers. They have presented a scenario where migration of holes from the YBCO into the LSMO converts a few unit cells of the latter into an antiferromagnet. This AF ordered layer pins the magnetic moment of the remaining ferromagnetic portion. Since the LSMO layer is on both sides of the YBCO, this effect should lead to two pinned magnetization vectors whose relative orientation can be anywhere from 0° to 180°. However, the observation of a net zero magnetization at H $<|H_s|$ demands that this angle is 180°. This is possible only when there is an exchange coupling across the YBCO. The magnetic behavior of ferromagnetic and antiferromagnetic LSMO couples has been studied in detail by Izumi *et al.*[40] for the case of $La_{0.6}Sr_{0.4}MnO_3/La_{0.45}Sr_{0.55}MnO_3$ superlattices, where the latter compound is a metallic A-type antiferromagnet. The Mn spins in alternate layers of this compound are coupled antiferromagnetically with their orientation in the [001] plane. Izumi *et al.*[40] note that the magnetization of the ferromagnetic layers is perpendicular to the magnetic easy axis of the antiferromagnetic layer, thus ruling out exchange biasing. While the measurement of far-infrared conductivity $\sigma_1(\omega)$ of YBCO-LSMO multilayers by Holden *et al.*[41] does show a strong suppression of the free-carrier contribution to $\sigma_1(\omega)$, migration of holes is only one of the possible mechanisms proposed by them for the suppression. Further, keeping in view the result of Izumi *et al.*,[40] a possible hole transfer does not *a priori* imply exchange biasing. In order to check if there is any exchange biasing effect of the interfacial LSMO in our trilayers, we have plotted a minor loop for a sample with $d_Y = 100$ Å. Starting from saturation magnetization in the forward direction, the field was decreased to a value $|H| < |H_s|$ in the negative direction and then increased again. In the presence of exchange biasing, the minor loop obtained in this way should be shifted along the field axis by an amount equal to the biasing field. However, the minor loop in Fig. 8 shows no shift within an accuracy of 5 Oe.

Noting that the hysteresis seen in Figs. 6 and 7 is a signature of antiferromagnetic coupling between the LSMO layer magnetizations, we now proceed to estimate the exchange energy and its temperature dependence. The free-energy expression for two magnetic layers of equal thickness coupled by bilinear coupling can be written as[42]

$$F = F_c + F_a - \vec{H} \cdot (\vec{M}_1 + \vec{M}_2)t, \qquad (2)$$

where $\vec{M}_1$ and $\vec{M}_2$ are the magnetizations of the top and bottom LSMO layers, $F_c$ is the coupling energy per unit area, and $t$ is the thickness of one LSMO layer. The anisotropy energy $F_a$ derives contributions from the magnetocrystalline anisotropy as well as in-plane uniaxial anisotropy of the film.
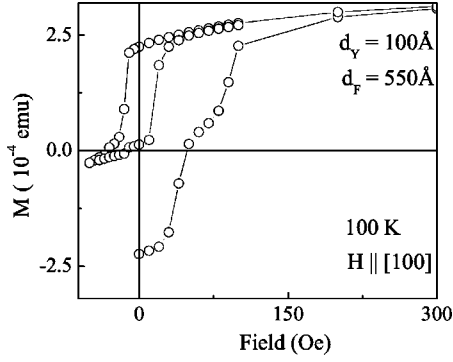
FIG. 8. The minor hysteresis loop (see the text for details) of a trilayer with a 100 Å YBCO layer sandwiched between 550 Å LSMO layers on both sides is shown superposed on the main magnetization curve. The measurement was performed at 100 K after cooling the sample in zero field.

Under the assumption of a bilinear coupling, $F_c$ can be written as

$$F_c = -J_1(\hat{M}_1 \cdot \hat{M}_2).\tag{3}$$

Here $\hat{M}_1$ and $\hat{M}_2$ are unit magnetization vectors, and $J_1 < 0$ corresponds to antiferromagnetic coupling between the FM layers. The equilibrium orientation of $\vec{M}_1$ and $\vec{M}_2$ is found by minimization of the free energy with respect to variations in the orientations of these two vectors. In a special case, when the interlayer exchange $J_1(\hat{M}_1 \cdot \hat{M}_2)$ is $< F_a$, the magnetization increases slowly in small field and then at a critical value of the field jumps to the saturation $M_s$. The switching field $H_s$ in this case for magnetic layers of equal thickness ($t$) and magnetization density ($M_s$) is written as

$$H_s = -(J_1/M_s t).\tag{4}$$

The behavior of magnetization seen in Figs. 5–7 corresponds to this situation. We have made an estimate of $J_1$ from the measured $H_s$ and magnetization density $M_s$ using Eq. (4). Figure 9 shows the variation of $J_1$ as a function of temperature for trilayers of different YBCO layer thickness. In the figure, we note that the coupling energy at $T > T_c$ is small, nonoscillatory, and decreases exponentially with the thickness of the superconductor. In all cases, however, $J_1$ increases monotonically as the temperature is lowered to $T_c$. Below this temperature, a truncation of the monotonic growth of $J_1$ is evident in all samples.

The temperature dependence of the interlayer exchange coupling in metallic multilayers has been worked out theoretically.[43,44] Following Bruno,[44] the amplitude of the linear exchange coupling coefficient $J_1$ increases with the decreasing temperature in the following manner:

$$J_1(T) = J_1(0)\left(\frac{T/T_0}{\sinh T/T_0}\right),\tag{5}$$

where the characteristic temperature $T_0$ depends on Fermi wave vector $k_F$ and spacer thickness $d_n$ through the relation $T_0 = \hbar k_F/2\pi k_B d_n m$, where $m$ is the free-electron mass and $\hbar$ and $k_B$ are Planck and Boltzmann constants, respectively.
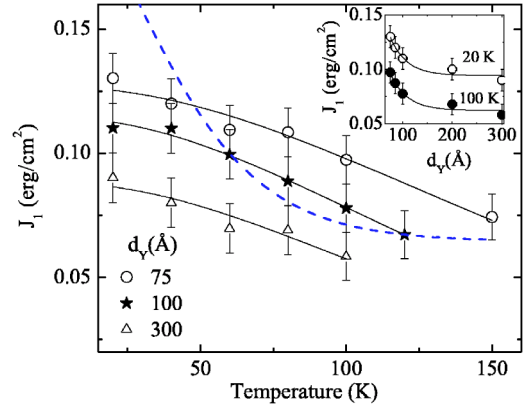


FIG. 9. (Color online) The antiferromagnetic coupling energy ($J_1$) calculated using the relation $|J_1| = H_s M_s t$ [Eq. (4)] is shown as a function of temperature for three sandwich structures with YBCO thickness of 75 Å (○), 100 Å (⋆), and 300 Å (△) and a constant LSMO thickness of 300 Å. The solid lines are fits to the equation $J_1 \sim (T/T_0)/\sinh(T/T_0)$ (Ref. 44). The dashed line is a theoretically generated curve showing how $J_1$ should grow with respect to the value at 120 K if $k_{F_Z}$ is taken to be $\pi/2c$, where $c$ is the $c$-axis lattice parameter (see text for details). Inset: the dependence of $J_1$ on the thickness of the YBCO spacer is plotted at 20 K and 100 K. A characteristic decay length of ~150 Å was obtained by fitting these data to a first-order exponentially decaying function (shown as the solid lines).

The calculations of Edwards et al.[43] also yield a similar temperature dependence of $J_1$. Since the transport in the present case is along the $c$ axis of the YBCO, the relevant Fermi wave vector is $k_{F_Z} = \pi/2c$, where $c$ is the $c$-axis lattice parameter (~12 Å).[10] We have fitted the temperature dependence of $J_1$ shown in Fig. 9 to Eq. (5). However, the average value of $k_{F_Z}$ obtained from these fits is larger by a factor of ~4 compared to the $k_{F_Z}$ expected for YBCO.[10] In Fig. 9, we show a theoretical curve for $J_1(T)$ generated using Eq. (5) with $k_{F_Z} = \pi/2c$, $d_Y = 100$ Å, and $J_1(T)$ such that the experimental and calculated values of $J_1$ at 120 K are the same. The calculated $J_1(T)$ shows a steep increase at the lower temperatures where the experimental data reach saturation. This truncation of the theoretically expected growth of $J_1$ below $T_c$ is suggestive of a superconducting gap.

### IV. DISCUSSION

Although the physics of magnetic coupling across a superconducting spacer of anisotropic order parameter is an enormously complicated problem to analyze, the following arguments can be made on the basis of the data shown in Fig. 5 through Fig. 9. We first consider the case when YBCO is in the normal state. The coupling in this situation is mediated by the transport of carriers perpendicular to $CuO_2$ planes in these $c$-axis-oriented films. While the resistivity of YBCO along the $c$-axis shows a variety of behaviors depending on doping concentration and defect structure, for optimally doped YBCO it is metallic, but larger by a factor of ~50 compared to the in-plane resistivity.[45] The $c$-axis transport in optimally doped and overdoped YBCO involves blocking of

coherent interplanar tunneling by the in-plane scattering. This leads to $\rho_c \propto \rho_{ab}$.[46,47] In underdoped systems, diffusive tunneling dominates the transport, leading to a semiconductorlike resistivity.[48] The nonoscillatory and predominantly antiferromagnetic IEC seen here is analogous to the behavior of exchange coupling in Fe-FeSi-Fe (Ref. 49) and Fe-Si-Fe (Ref. 50) heterostructures. The IEC in this case is strongly antiferromagnetic ($J_1 \sim 2$ erg/cm$^2$) for a thin spacer, and decays exponentially with the increasing spacer thickness. Furthermore, the exchange energy $J_1$ shows a monotonic drop with the increasing temperature, a behavior similar to the data shown in Fig. 9. A bias towards antiferromagnetic IEC has been predicted theoretically as well. Shi, Levy, and Fry[51] have shown that this bias for AF-coupling arises from a competition between the RKKY-like exchange and superexchange, and a noncancellation of the nonoscillatory parts of these two contributions. An AF coupling, which decays exponentially with the spacer thickness, has been predicted by Slonczewski[52] and Bruno[44] using an electron tunneling picture. The theory[44] predicts a $d_n$ dependence of the type $J_1 \sim (1/d_n^2)\exp(-d_n/\lambda)$. The calculated value of the coupling energy $J_1$ for our trilayers is plotted in the inset of Fig. 9 as a function of the spacer layer thickness. We have fitted these data to a first-order exponential decay of the type given by Bruno *et al.*[44] Results of this fitting are shown as solid lines in the inset. The characteristic decay length $\lambda$ inferred from the fit is $\sim 150$ Å. Since the $c$-axis transport in YBCO is controlled by a delicate balance between single electron tunneling and intralayer electron-electron scattering processes,[46–48] a tunneling picture for IEC is applicable, albeit with the caveat that it is unlike the tunneling through a semiconducting barrier where thermally induced carriers can enhance IEC at higher temperatures.[44] The IEC in this case is expected to decay with temperature as the $c$-axis resistivity shows a linear temperature dependence.

The truncation of the monotonic growth of the exchange coupling energy when the YBCO layer becomes superconducting (as seen in Fig. 9) is in agreement with the predictions of Šipr and Györffy[8] and of de Melo.[9] However, the extent of the drop in the coupling energy in the $T=0$ limit depends on the strength of the superconducting gap parameter. For a weak ferromagnet and an isotropic superconductor, de Melo[9] has derived an analytic expression for the effective coupling Hamiltonian,

$$H_{eff} \sim \frac{\cos(2k_F d_s)}{(2k_F d_s)^2} \exp\left(-\frac{k_F d_s \Delta}{E_F}\right), \qquad (6)$$

where $k_F$ and $d_s$ are the Fermi momentum and thickness of the S-layer, respectively. $\Delta$ is the superconducting gap and

$E_F$ is the Fermi energy. This expression shows that the superconducting order does not actually contribute to the oscillating part of the interaction, it only induces a relative decrease in the strength of interaction as compared to the interaction for a normal metallic spacer. However, the low-temperature calculations in Refs. 8 and 9 are valid only for an isotropic gap parameter. de Melo has recently considered the case of IEC through a d-wave superconductor whose order parameter lies in the plane of the multilayer.[10] The main contribution to coupling in this case comes from the wave vectors connecting points at the Fermi surface along the [001] direction and for $\vec{k}_\parallel$ lying along the direction of nodes. A distinct suppression, although not as much as in the case of a fully gapped system, has been seen in the superconducting state.

## V. CONCLUSIONS

In summary, we have studied the magnetic and superconducting states of epitaxial thin film heterostructures consisting of two La$_{0.67}$Sr$_{0.33}$MnO$_3$ layers separated by a layer of YBa$_2$Cu$_3$O$_7$, whose $c$ axis is perpendicular to the plane of the heterostructure. We see a distinct influence of the ferromagnetic boundaries on the $T_c$ of the YBCO layer. This is attributed to the pair-breaking phenomena near the F-S interface. The hysteresis loops for in-plane magnetization of the heterostructures show signatures of an antiferromagnetic coupling between the moments of the two LSMO layers in the superconducting as well as the normal state of the spacer. The temperature dependence of the exchange coupling energy shows a monotonic growth followed by saturation on lowering the temperature. The long-range coupling was found to decrease exponentially with the increasing thickness of the spacer layer. The suppression of $J_1$ at $T < T_c$ suggests inhibition of single-electron tunneling along the $c$ axis of YBCO as the in-plane superconducting order parameter becomes nonzero.

---

*Electronic address: rcb@iitk.ac.in

[1] See, for example, *Ultrathin Magnetic Structures II*, edited by B. Heinrich and J. A. C. Bland (Springer-Verlag, Berlin, 1994).

[2] P. Grunberg, R. Schreiber, Y. Pang, M. B. Brodsky, and H. Sowers, Phys. Rev. Lett. **57**, 2442 (1986).

[3] M. N. Baibich, J. M. Broto, A. Fert, F. Nguyen Van Dau, F. Petroff, P. Etienne, G. Creuzet, A. Friederich, and J. Chazelas, Phys. Rev. Lett. **61**, 2472 (1988).

[4] S. S. P. Parkin, N. More, and K. P. Roche, Phys. Rev. Lett. **64**, 2304 (1990).

[5] A. Orozco, S. B. Ogale, Y. H. Li, P. Fournier, Eric Li, H. Asano, V. Smolyaninova, R. L. Greene, R. P. Sharma, R. Ramesh, and

T. Venkatesan, Phys. Rev. Lett. **83**, 1680 (1999).

[6] K. R. Nikolaev, A. Yu. Dobin, I. N. Krivorotov, W. K. Cooley, A. Bhattacharya, A. L. Kobrinskii, L. I. Glazman, R. M. Wentzovitch, E. D. Dahlberg, and A. M. Goldman, Phys. Rev. Lett. **85**, 3728 (2000).

[7] P. Padhan, R. C. Budhani, and R. P. S. M. Lobo, Europhys. Lett. **63**, 771 (2003).

[8] O. Šipr and B. L. Györffy, J. Phys.: Condens. Matter **7**, 5239 (1995).

[9] C. A. R. Sá de Melo, Phys. Rev. Lett. **79**, 1933 (1997); Phys. Rev. B **62**, 12 303 (2000).

[10] C. A. R. Sá de Melo, Physica C **387**, 17 (2003).

[11] J. J. Hauser, H. C. Theuerer, and N. R. Werthamer, Phys. Rev. **142**, 118 (1966).

[12] H.-U. Habermeier, G. Cristiani, R. K. Kremer, O. Lebedev, and G. van Tendeloo, Physica C **364–365**, 298 (2001).

[13] Z. Sefrioui, D. Arias, V. Peña, J. E. Villegas, M. Varela, P. Prieto, C. León, J. L. Martinez, and J. Santamaria, Phys. Rev. B **67**, 214511 (2003).

[14] B. S. H. Pang, R. I. Tomov, and M. G. Blamire, Semicond. Sci. Technol. **17**, 624 (2004).

[15] Z. W. Dong, R. Ramesh, T. Venkatesan, M. Johnson, Z. Y. Chen, S. P. Pai, V. Talyanski, R. P. Sharma, R. Shreekala, C. J. Lobb, and R. L. Greene, Appl. Phys. Lett. **71**, 1718 (1997).

[16] A. M. Goldman, V. Vasko, P. Kraus, K. Nikolaev, and V. A. Larkin, J. Magn. Magn. Mater. **200**, 69 (1999).

[17] N. C. Yeh, R. P. Vasquez, C. C. Fu, A. V. Samoilov, Y. Li, and K. Vakili, Phys. Rev. B **60**, 10 522 (1999).

[18] G. Jacob, V. V. Moshchalkov, and Y. Bruynseraede, Appl. Phys. Lett. **66**, 2564 (1995).

[19] L. Fábrega, R. Rubi, V. Vrtik, C. Ferrater, F. Sánchez, M. Varela, and J. Fontcuberta, J. Magn. Magn. Mater. **211**, 180 (2000).

[20] P. Przyslupski, I. Komissarov, W. Paszkowicz, P. Dluzewski, R. Minikayev, and M. Sawicki, Phys. Rev. B **69**, 134428 (2004).

[21] Yan. Wu, Y. Suzuki, U. Rüdiger, J. Yu, A. D. Kent, T. K. Nath, and C. B. Eom, Appl. Phys. Lett. **75**, 2295 (1999).

[22] H. Y. Zhai and W. K. Chu, Appl. Phys. Lett. **76**, 3469 (2000).

[23] M. Kawasaki, K. Takahashi, T. Maeda, R. Tsuchiya, M. Shinohara, O. Ishiyama, T. Yonezawa, M. Yoshimoto, and H. Koinuma, Science **266**, 1540 (1994).

[24] K. Senapati and R. C. Budhani, Phys. Rev. B **70**, 174506 (2004).

[25] K. Senapati, S. Chakravarty, Leena K. Sahoo, and R. C. Budhani, Rev. Sci. Instrum. **75**, 141 (2004).

[26] C. Kittel, *Introduction to Solid State Physics*, 7th ed. (John Wiley and Sons, New York, 1996), p. 448.

[27] G. S. Rushbrooke and P. J. Wood, Mol. Phys. **1**, 257 (1958).

[28] Y. Suzuki, H. Y. Hwang, S.-W. Cheong, and R. B. van Dover, Appl. Phys. Lett. **71**, 140 (1997).

[29] K. Steenbeck and R. Hiergeist, Appl. Phys. Lett. **75**, 1778 (1999).

[30] A. M. Haghiri-Gosnet, J. Wolfman, B. Mercey, Ch. Simon, P. Lecoeur, M. Korzenski, M. Hervieu, R. Desfeux, and G. Baldinozzi, J. Appl. Phys. **88**, 4257 (2000).

[31] K. Steenbeck, T. Habisreuther, C. Dubourdieu, and J. P. Sénateur, Appl. Phys. Lett. **80**, 3361 (2002).

[32] A. Urushibara, Y. Moritomo, T. Arima, A. Asamitsu, G. Kido, and Y. Tokura, Phys. Rev. B **51**, 14 103 (1995).

[33] J.-M. Triscone and Ø. Fischer, Rep. Prog. Phys. **60**, 1673 (1997), and references therein.

[34] M. Varela, Z. Sefrioui, D. Arias, M. A. Navacerrada, M. Lucía, M. A. López de la Torre, C. León, G. D. Loos, F. Sánchez-Quesada, and J. Santamaría, Phys. Rev. Lett. **83**, 3936 (1999).

[35] T. Terashima, K. Shimura, Y. Bando, Y. Matsuda, A. Fujiyama, and S. Komiyama, Phys. Rev. Lett. **67**, 1362 (1991).

[36] W. E. Pickett, Phys. Rev. Lett. **78**, 1960 (1997).

[37] Z. Radovic, M. Ledvij, L. Dobrosavljevic-Grujic, A. I. Buzdin, and J. R. Clem, Phys. Rev. B **44**, 759 (1991).

[38] L. Lazar, K. Westerholt, H. Zabel, L. R. Tagirov, Yu. V. Goryunov, N. N. Garifyanov, and I. A. Garifullin, Phys. Rev. B **61**, 3711 (2000).

[39] P. Padhan and R. C. Budhani, Phys. Rev. B **71**, 144415(2005).

[40] M. Izumi, T. Manako, Y. Konishi, M. Kawasaki, and Y. Tokura, Phys. Rev. B **61**, 12 187 (2000).

[41] Todd Holden, H. U. Habermeier, G. Cristiani, A. Golnik, A. Boris, A. Pimenov, J. Humlicek, O. I. Lebedev, G. Van Tendeloo, B. Keimer, and C. Bernhard, Phys. Rev. B **69**, 064505 (2004).

[42] S. O. Demokritov, J. Phys. D **31**, 925 (1998).

[43] D. M. Edwards, J. Mathon, R. B. Muniz, and M. S. Phan, Phys. Rev. Lett. **67**, 493 (1991).

[44] P. Bruno, Phys. Rev. B **52**, 411 (1995).

[45] S. L. Cooper and K. E. Gray, in *Physical Properties of High Temperature Superconductors IV*, edited by D. M. Ginzburg (World Scientific, Singapore, 1994), pp. 61–188.

[46] N. Kumar and A. M. Jayannavar, Phys. Rev. B **45**, 5001 (1992).

[47] M. S. Kumar, S. Dattagupta, and N. Kumar, Phys. Rev. B **65**, 134501 (2002).

[48] M. Turlakov and A. J. Leggett, Phys. Rev. B **63**, 064518 (2001).

[49] J. J. de Vries, J. Kohlhepp, F. J. A. den Broeder, R. Coehoorn, R. Jungblut, A. Reinders, and W. J. M. de Jonge, Phys. Rev. Lett. **78**, 3023 (1997).

[50] G. J. Strijkers, J. T. Kohlhepp, H. J. M. Swagten, and W. J. M. de Jonge, Phys. Rev. Lett. **84**, 1812 (2000).

[51] Z. P. Shi, P. M. Levy, and J. L. Fry, Phys. Rev. B **49**, 15 159 (1994).

[52] J. C. Slonczewski, Phys. Rev. B **39**, 6995 (1989).